Article

Development of a Bedaquiline–Rifampicin Co-Amorphous Drug-Drug Delivery System for Tuberculosis Treatment

Nadica Karakamisheva , Péter Szabó , Sándor Nagy , Tomislav Balić , Edina Szabó , Szilárd Pál , Aleksandar Széchenyi , Ala' Salem *

Posted Date: 16 April 2026

doi: 10.20944/preprints202604.1177.v1

Keywords: bedaquiline fumarate; rifampicin; fumaric acid; tuberculosis; dissolution; drug-interactions; drug-drug co-amorphous delivery system; poorly soluble drugs; co-amorphous systems

 doi:10.20944/preprints202604.1177.v1

Article

Development of a Bedaquiline–Rifampicin Co-Amorphous Drug-Drug Delivery System for Tuberculosis Treatment

Nadica Karakamisheva [1], Péter Szabó [2,3], Sándor Nagy [1], Tomislav Balić [4], Edina Szabó [5], Szilárd Pál [1], Aleksandar Széchenyi [1,4] and Ala' Salem [6,*]

[1] Institute of Pharmaceutical Technology and Biopharmacy, University of Pécs, Pécs, Hungary
[2] Environmental Analytical and Geoanalytical Research Group, Szentágothai Research Centre, University of Pécs, Pécs, Hungary
[3] Institute of Geography and Earth Sciences, University of Pécs, Pécs, Hungary
[4] Department of Chemistry, Josip Juraj Strossmayer University of Osijek, Osijek, Croatia
[5] Department of Organic Chemistry and Technology, Faculty of Chemical Technology and Biotechnology, Budapest University of Technology and Economics, Műegyetem rkp. 3., H-111 Budapest, Hungary
[6] Pharmacy Department, Faculty of Health Science Social Care and Education, Kingston University London, London, UK
* Correspondence: a.salem@kingston.ac.uk

Abstract

Tuberculosis remains a major cause of mortality globally. Treatment of tuberculosis requires a long duration with multiple drug regimen. Unfortunately, tuberculosis drug resistance is emerging, resulting in a treatment failure rate of 14% in new cases. Bedaquiline, a poorly soluble second-line drug is used to treat multidrug-resistant tuberculosis in combination with first-line anti-tuberculosis drugs. Bedaquiline is often administered with rifampicin, as this combination has demonstrated additive intracellular bactericidal and faster onset of action compared to bedaquiline monotherapy. However, co-administration with rifampicin has been reported to increase bedaquiline clearance, reducing concentration of bedaquiline in the blood by up to 25%. There is a need for alternative pharmaceutical formulations to enhance bedaquiline bioavailability and treatment success of tuberculosis. Co-amorphous drug delivery systems have the potential to improve the water solubility and bioavailability of poorly soluble drugs. In an aim to enhance the solubility of bedaquiline when co-administered with rifampicin, we have prepared co-amorphous systems of rifampicin and bedaquiline fumarate. First, miscibility of the components was assessed using Hansen solubility parameters. Then, the solid co-amorphous drug was prepared by fast solvent evaporation, and characterized using PXRD, TGA-DSC, FTIR, dissolution rate, and accelerated stability study. Results show that the co-amorphous form exhibited better dissolution for bedaquiline without compromising rifampicin dissolution. Furthermore, the co-amorphous product remained stable under stress conditions for 30 days. These findings suggest that co-amorphous systems of rifampicin and bedaquiline fumarate may represent a viable strategy to improve treatment outcomes for patients with multidrug-resistant tuberculosis treated with these drugs and decrease pill burden.

Keywords: bedaquiline fumarate; rifampicin; fumaric acid; tuberculosis; dissolution; drug-interactions; drug-drug co-amorphous delivery system; poorly soluble drugs; co-amorphous systems

1. Introduction

Tuberculosis (TB) is an infectious disease, mainly affecting the lungs. TB is primarily caused by *Mycobacterium tuberculosis* and other closely related bacteria. This single infection caused mortality in 1.28 million infected people in 2020, and 1.3 million in 2022, making it a global public health concern

 doi:10.20944/preprints202604.1177.v1

[1]. Following infection, clinical manifestations can vary widely, ranging from asymptomatic cases to life-threatening illness. The disease usually presents itself as pulmonary TB, however it may spread and be represented as extrapulmonary TB [2]. The treatment of TB necessitates the use of multiple first-line antibiotics (rifampicin, isoniazid, pyrazinamide, and ethambutol) for a long period [3]. Treatment duration and regimen depend on factors such as severity, patient age and the type of TB infection. The short-term treatment option consists of a 4-month combination therapy: 2 months of isoniazid-rifampicin-pyrazinamide-ethambutol, followed by 2 months of isoniazid-rifampicin. Long period therapy of 10 or more months is administered in the case of the long-term treatment of extrapulmonary TB affecting the central nervous system [4].

Multidrug resistance of the bacterium has been reported in patients receiving first-line combination therapy. In a 10-year study by Desikan *et al*. [5] with a total of 28,814 samples from India, 5.86% were multidrug resistant. The combination of existing and new drugs is being tested to shorten the treatment duration and treat multidrug-resistant TB. Furthermore, the treatment of TB has advanced with the introduction of the new drugs bedaquiline and delamanid [6].

Bedaquiline is highly effective against multidrug-resistant tuberculosis. Its antimycobacterial action is achieved by blocking ATP generation, which is essential for both *Mycobacterium* TB growth and survival in its latent, non-growing form. Specifically, bedaquiline targets and interferes with mycobacterial F-ATP synthase activity, inhibiting ATP synthesis, leading to depletion of intracellular ATP and, ultimately, bacterial death. Notably, bedaquiline exhibits delayed bactericidal activity, meaning that cell death does not occur immediately following ATP depletion [7]. However, bedaquiline has been reported as poorly soluble in water . To improve its solubility and bioavailability, bedaquiline is formulated as a fumarate salt [8]. Bedaquiline fumarate salt displays a high packing efficiency, featuring multiple strong hydrogen bonds; and augmented by other weaker directional interactions, including C-H···O and C-H···Br bonds, creating a three-dimensional structure of interconnected ribbons. These ribbons further interact with neighboring segments, stabilizing the structure. Moreover, the salt lacks unoccupied void space or incorporated solvent molecules [8]. Unfortunately, strains resistant to bedaquiline have been reported and caused additional concerns regarding its use in TB treatment. Traditional treatment plans for multidrug-resistant TB are no longer the solution because research has shown that using a combination of second-line medications for at least 20 months is not only costly and ineffective compared to using drugs to treat drug-susceptible TB, but is also harmful. Only 50% of the patients receiving conventional therapy responded well to it, based on a cohort study [9].

Rifampicin, a semisynthetic derivative of rifamycin, was introduced as an anti-TB medication in 1972 [10]. It selectively inhibits bacterial RNA polymerase, the enzyme responsible for DNA transcription [11]. The majority of cases (95%) of rifampicin resistance are genetically caused by mutations in the 81-base pair rifampicin resistance-determining region of the rpoB gene of *Mycobacterium tuberculosis*. Rifampicin resistance often develops in a single step [10]. The resistance is often overcome by using a drug combination with different mechanisms of action.

Combination of bedaquiline with rifampicin demonstrated additive intracellular bactericidal and faster onset of action compared to bedaquiline monotherapy in *ex vivo* whole-blood cultures from healthy volunteers. These findings suggest that incorporating bedaquiline could substantially enhance early-phase bacillary clearance in TB regimens [12]. However, the use of drug combinations always raises the question of drug interactions. The chemical structures of bedaquiline, rifampicin and fumaric acid are shown in **Figure 1**.

 doi:10.20944/preprints202604.1177.v1

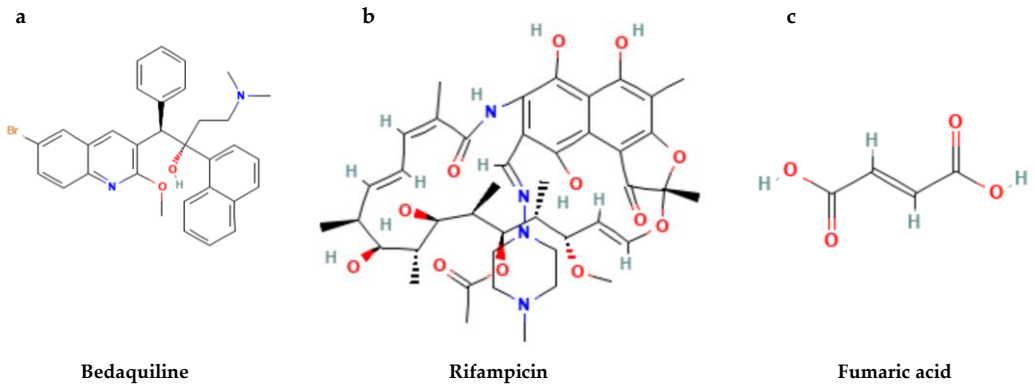

Figure 1. Chemical structure of (a) bedaquiline; (b) rifampicin; and (c) fumaric acid, structures from PubChem.

The co-administration of bedaquiline and rifampicin was studied in detail on healthy volunteers [13]. It was found the cytochrome P450 3A4 enzyme catalyzes the primary N-demethylation process that breaks down the cationic amphiphilic drug bedaquiline. When compared to bedaquiline, the resultant metabolite, N-monodesmethyl-bedaquiline (M2) [13], is three to six times less active *in vitro*. Additionally, studies indicate that M2 may induce phospholipidosis and cytotoxicity at lower concentrations than the parent medication. However, in humans, M2 circulates at significantly lower quantities than the parent medication, and there is a lack of information on the clinical exposure-response linkages for both safety and efficacy between M2 and bedaquiline. A study by Svensson *et al.* [13] was carried out to evaluate how administering rifampicin affected the safety, tolerability, and pharmacokinetics of bedaquiline and M2. Potentially, with proper adjustments of the dosage, it is possible to diminish effect of the interaction between the two active pharmaceutical ingredients (APIs). However, this could result in an overpriced treatment option with uncertain safety. Although rifampicin is a potent inducer of cytochrome P450 3A4 and is known to reduce bedaquiline plasma levels with repeated dosing, emerging evidence from single-dose co-administration studies in leprosy prophylaxis [14][15], suggests that this interaction may be minimal when administered as a one-time treatment. This finding opens the possibility for safely exploring co-administration strategies in TB therapy [16] before optimizing effective long-term drug therapy.

There is a growing need for alternative pharmaceutical formulations to enhance treatment success of TB [16]. Co-amorphous drug delivery systems have presented a promising alternative to surpass the issue of poorly soluble drugs. These systems are composed of low molecular mass drugs and a co-former, in a homogenously distributed amorphous mixture. Drug-drug co-amorphous systems have provided a significant improvement in dissolution and stability. Moreover, they are a potential alternative to development of combined treatment options [17]. The beginning of characterization of these systems was the initial discovery of binary glass complex by Fukuoka *et al*. [18] in 1989. In the case of binary systems, more so often the bioavailability of a drug is poorly enhanced, therefore, to overcome this issue, a third component is incorporated in the system either as internal or external [19]. Enhancement of the dissolution of a drug is obtained by supersaturation which could potentially lead to enhanced oral bioavailability [17].

The aim of this study is to prepare rifampicin and commercially available bedaquiline fumarate ternary co-amorphous drug-drug delivery system and examine the potential dissolution advantages of this formulation, which may enhance the potential of this combination for treatment of multidrug-resistant TB. Essentially, this study aims to enhance the dissolution of bedaquiline using a drug-drug co-amorphous delivery system to offset the increased clearance caused by co-administration with rifampicin.

 doi:10.20944/preprints202604.1177.v1

2. Materials and methods

2.1. Materials

Rifampicin (95%) and bedaquiline fumarate (98.5%) were purchased from Acros organics (Fair Lawn, NJ, USA). HPLCgrade acetonitrile was supplied from VWR (Radnor, PA, USA) chemicals and 37% hydrochloric acid from Carlo Erba reagents (Val-de-Reuil, France). All materials were used as received.

2.2. Methods

2.2.1. Co-amorphous system formation screening and solvent selection

Hansen solubility parameters (HSPs) were used to establish the potential of miscibility of components and guide the selection of a suitable solvent for co-amorphous system formation. Hansen solubility parameters were adapted from Hildebrand parameters (δ), which show potential incompatibilities between drugs and carriers in solid dispersions. Hansen solubility parameters were further adapted to predict polymer mixing, mixing of nanostructured materials[20] and formation of pharmaceutical cocrystals[21]. Here we have stretched the use of Hansen solubility parameters to screen the likelihood of formation of co-amorphous system. Hansen solubility parameters are made of contributions from atomic dispersion (δ_d), polarity (δ_p) and hydrogen-bonding contributions (δ_h). These contributions might predict interactions in and between materials more accurately and might show potential incompatibilities more accurately [22]. The suggested cut-off values are Δδ at 8.18, $\Delta\delta_t$ at 16.87 and Ra at 17.64 $MPa^{0.5}$ [22]. HSPiP software (version 5.3.08) was used to calculate Hansen solubility parameters of the drugs. According to previously published work [19], the calculated modified radius (Ra) value of 2.0 $MPa^{0.5}$ (**Table 1**) indicates that rifampicin and bedaquiline were within the range of mixability (Ra value less than 17.64 $MPa^{0.5}$). On the other hand, the Ra value between rifampicin and fumaric acid (20.9 $MPa^{0.5}$) is above the cut-off value for miscibility. However, as bedaquiline is commercially available as the fumaric acid salt, the fumaric acid would dissociate and we expect the APIs to interact and form a co-amorphous system. Solvent selection was also done based on Hansen Solubility Parameters calculations. An appropriate solvent would have near equal miscibility with the two APIs [23]. The Hansen solubility parameters of a total of eight solvents (ethanol, 2-propanol, methyl acetate, ethyl acetate, acetone, iso-propyl acetate, acetonitrile and methanol) were calculated using HSPiP software (version 5.3.08) and compared to the Hansen solubility parameters of rifampicin and bedaquiline (**Table S1**) to select a suitable solvent. Furthermore, both bedaquiline and rifampicin are prone to form solvates, but there are no known solvates with acetonitrile. Therefore, only the aprotic solvent acetonitrile was selected for this study.

Table 1. Hansen solubility parameters and co-formability prediction calculations vs rifampicin.

API	δ_d	δ_p	δ_h	δ	δ_{hDon}	δ_{hAcc}	Ra	Δδ	$\Delta\delta_{tot}$
Rifampicin	20.0	3.4	3.8	20.6	0.3	1	-	-	-
Bedaquiline	20.5	3.4	5.6	21.5	1.5	5.8	2.0	0.9	1.8
Fumaric acid	18.16	10.78	23.02	30.2	18.8	13.2	20.9	10.6	20.6

Values reported in ($MPa^{0.5}$). (δ_d) atomic dispersion contribution of Hansen solubility parameters; (δ_p) polarity contribution of Hansen solubility parameters; (δ_h) hydrogen-bonding contribution of Hansen solubility parameters; (δ) total Hansen solubility parameters; (δ_{hDon}) hydrogen-bond donation contribution of Hansen solubility parameters; (δ_{hAcc}) hydrogen-bond acceptance contribution of Hansen solubility parameters; (Ra) Difference between the rifampicin and bedaquiline/fumaric acid Hansen parameters in the modified radius (Ra) in Hansen space; (Δδ) Absolute solubility difference between rifampicin and bedaquiline/fumaric acid; ($\Delta\delta_{tot}$) Three dimensional point representation difference in solubility between rifampicin and bedaquiline/fumaric acid.

 doi:10.20944/preprints202604.1177.v1

2.2.2. Co-amorphous Drug Delivery System Preparation

Fast solvent evaporation method was used to prepare the co-amorphous drug-drug system [17]. Briefly, bedaquiline fumarate and rifampicin were dissolved in acetonitrile in a 1:1 molar ratio. The resulting solution was then sonicated (RK Tech, USA) for 3 minutes until complete dissolution. The solvent was evaporated using a rotary evaporator Laborota 4000 (Heidolph, Schwabach, Germany) attached to a vacuum pump to prepare the co-amorphous system. The rotation speed was set to 90 rpm and the temperature was set to 45±1°C. Samples were placed in a desiccator (JEOL, Tokyo, Japan) before further analysis.

2.2.3. Scanning Electron Microscopy

Sample images were captured using a scanning electron microscope (SEM, JEOL JSM-IT500HR, Japan). Samples were coated with gold using an auto fine coater (JEOL JFC-1300 auto fine coater, Japan), then placed on double-sided carbon tape. For the imaging the secondary electron mode was used and the accelerating voltage was set to 5kV.

2.2.4. Powder X-Ray Diffraction

The samples were characterized by powder X-ray diffraction (PXRD). Powder samples were placed in an aluminum sample holder and gently pressed with a glass slide to obtain a flat surface. Consequently, they were analyzed by Rigaku MiniFlex 600 X-ray diffractometer (Rigaku, Japan) at room temperature using Cu-Kα1 radiation and Smart lab/MiniFlex guidance software (version 2.0.2.1) to obtain PXRD patterns. Data was collected in the 5–35° 2θ range at a 3°/min scanning rate and a step size of 0.02°.

2.2.5. Differential Scanning Calorimetry-Thermogravimetric Analysis

Mettler Toledo DSC coupled TGA 821e (Mettler Toledo, USA) and STARe Evaluation software (version 11) were used to obtain the thermographs. Samples were placed into aluminum pans, which were then sealed and pierced to provide vent holes. A heating rate of 10 °C/min and temperature range of 30–300°C under nitrogen purge were used. All reported temperatures refer to the melting onset.

2.2.6. Modulated Differential Scanning Calorimetry-MDSC Analysis

Mettler Toledo DSC3+ device (Mettler Toledo AG, Zürich, Switzerland) coupled with a Huber TC100 cooler (Offenburg, Germany) was used to examine the phase transitions of co-amorphous product. The measurements were performed in a stochastic temperature-modulated mode TOPEM®, for separation of the total heat flow to reversing- and non-reversing components. The frequency range of modulation was set to 15 and 30s, while the temperature was raised from 25°C to 175°C with overall heating rate of 2°C/min. The Measurements were performed in nitrogen stream 50mL/h, with sample weight of 10.44 mg in aluminum pan.

2.2.7. Fourier-Transform Infrared Spectroscopy

Fourier-transform infrared spectroscopy spectral analysis was performed using Nicolet 380 FTIR spectrometer (Thermo Fisher, USA). Powder samples were placed on the sample holder and slightly pressed with a spatula to obtain a flat surface. Data was collected in the 4000-400 cm^{-1} range and 4 cm^{-1} resolution. Omnic software (version 9.2) was used to record the IR absorbance.

2.2.8. Dissolution Study

Dissolution study was carried out using dissolution apparatus (ERWEKA DT 700, Erweka, Langen, Germany) with 0.01 M HCl as simulated gastric media at 37°C and 50 rpm. Samples of 5 mL were drawn, by an automatic sampler (Hanson Research, Microette Plus, USA) with an attached 1 µ

 doi:10.20944/preprints202604.1177.v1

polyethylene canula filter (PSFIL001-EW-100, Erweka), at 5, 10, 20, 30, 45, and 60 minutes and analyzed by UV/Vis spectrophotometer (Jasco V-670, USA) at 255 and 334 nm. The multi-wavelength linear regression method was used to account for the overlapping absorbance. The multi-wavelength linear regression method is a chemometric technique used to deconvolute overlapping UV/Vis spectra by leveraging absorbance data across multiple wavelengths. In mixtures where several drugs contribute to the total absorbance, this method assumes that the absorbance at each wavelength is a linear combination of the individual contributions from each drug, based on their known molar absorptivities. By measuring the absorbance of the mixture at several wavelengths and using reference spectra of the pure components, a system of linear equations was constructed. Solving this system using linear regression allows for the estimation of the concentrations of each drug in the dissolution media. This approach is particularly useful when spectral overlap makes traditional single-wavelength analysis unreliable, and it enhances accuracy by utilizing the full spectral profile rather than isolated peaks. [24]. Further details of the dissolution study, including calibration curves are presented in the Supplementary Materials (**Figures S1–S3**).

2.2.9. Accelerated Stability Study

The accelerated stability test was performed for 30 days. Temperature was set at 40°C and humidity 75%, according to the Food and Drug Administration guidelines [25]. The PXRD patterns of the sample were analyzed to examine the stability before and after the accelerated stability study.

2.2.10. Statistical Analysis

Statistical analysis was carried out using one-tailed two-sample t-test using IBM SPSS (software version 25 IBM, NY, USA) and Microsoft Excel 2016 (version 16.0.5356.1000). A p-value of ≤0.05 was considered statistically significant. All values are expressed as mean ± standard deviation (SD) of triplicate (n = 3) measurements.

3. Results and Discussion

3.1. Morphology and Solid-State Characterization

3.1.1. Morphology by Scanning Electron Microscopy

The surface morphology of the samples was examined by SEM. Rifampicin appeared as a rod-like crystals (**Figure 2a**), consistent with the observation reported previously [26]. Bedaquiline fumarate had smooth flake-like surfaces (**Figure 2b**), in agreement with previously described morphology [27]. The co-amorphous product appeared to have sharp edges and irregular shapes, with randomly oriented surfaces and edges indicative of a glassy structure typical for an amorphous solid (**Figure 2c**). Fast solvent evaporation of rifampicin with bedaquiline fumarate yielded a co-amorphous mass with a low percentage of crystalline byproducts.

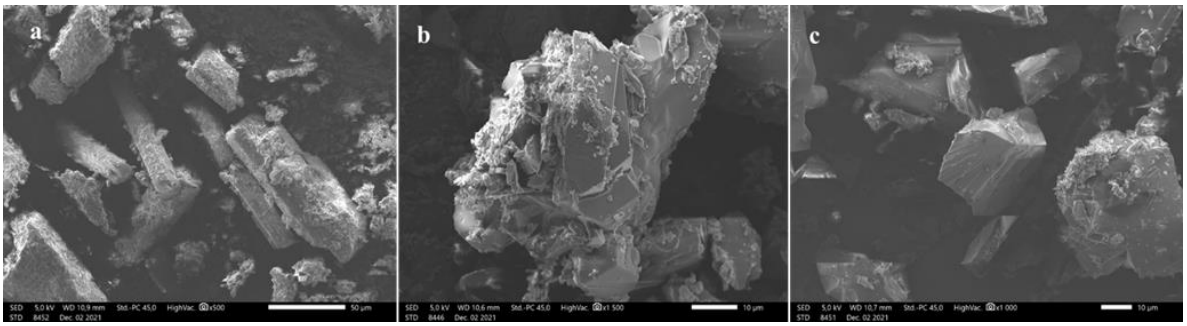

Figure 2. SEM photomicrographs of (**a**) rifampicin; (**b**) bedaquiline fumarate; and (**c**) rifampicin-bedaquiline fumarate co-amorphous product.

 doi:10.20944/preprints202604.1177.v1

3.1.2. Powder X-Ray Diffraction Patterns

PXRD patterns were obtained to characterize the structure of the samples. The PXRD patterns indicate the formation of amorphous material (**Figure 3**). Peaks characteristic of bedaquiline fumarate around 10.58, 14.3, and 23.39° [28] and rifampicin at 16.4, and 20.48° [26] are absent in the PXRD patterns of the co-amorphous system. Furthermore, only broad halos consistent with amorphous rather than crystalline material can be observed [29]. It is worth mentioning that the acetonitrile solvate of the bedaquiline fumarate salt was reported to be unstable and converted into a form with similar PXRD patterns to that of a hydrate [8].

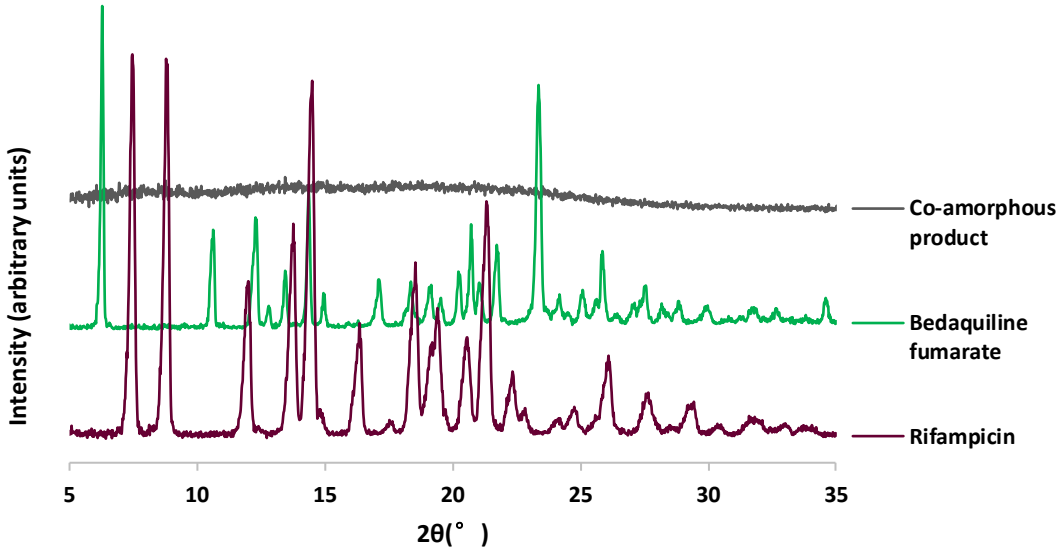

Figure 3. PXRD patterns of rifampicin, bedaquiline fumarate, and (CAMS) rifampicin-bedaquiline fumarate co-amorphous product.

3.1.3. Differential Scanning Calorimetry-Thermogravimetric Analysis Results

DSC-TGA thermograms of the samples are shown in **Figure 4a** and **Figure 4b**. Rifampicin was reported to have a melting endotherm at 180 °C [30]. Moreover, rifampicin's DSC profile is consistent with that of polymorph I, where no distinct fusion event was observed, with a thermal decomposition process occurring around 245 °C [31]. Bedaquiline fumarate showed a characteristic endothermic peak at 206.8 °C, similar to that reported at 208.48 °C [32], indicating consistent thermal properties. Furthermore, there are no distinct thermal events in the thermogram of the co-amorphous product (grey curves in **Figure 4a** and **b**) that could be related to the thermal events observed for pure rifampicin (polymorph I) and bedaquiline. This observation indicates formation of novel form. The slight shift from the baseline in the thermogram of the co-amorphous product at 160 °C (**Figure 4a**) could be interpreted as a glass-transition. However, this event also corresponds to the beginning of thermal decomposition of the co-amorphous product (grey curve in **Figure 4b**), therefore no final conclusion regarding glass-transition can be done.

 doi:10.20944/preprints202604.1177.v1

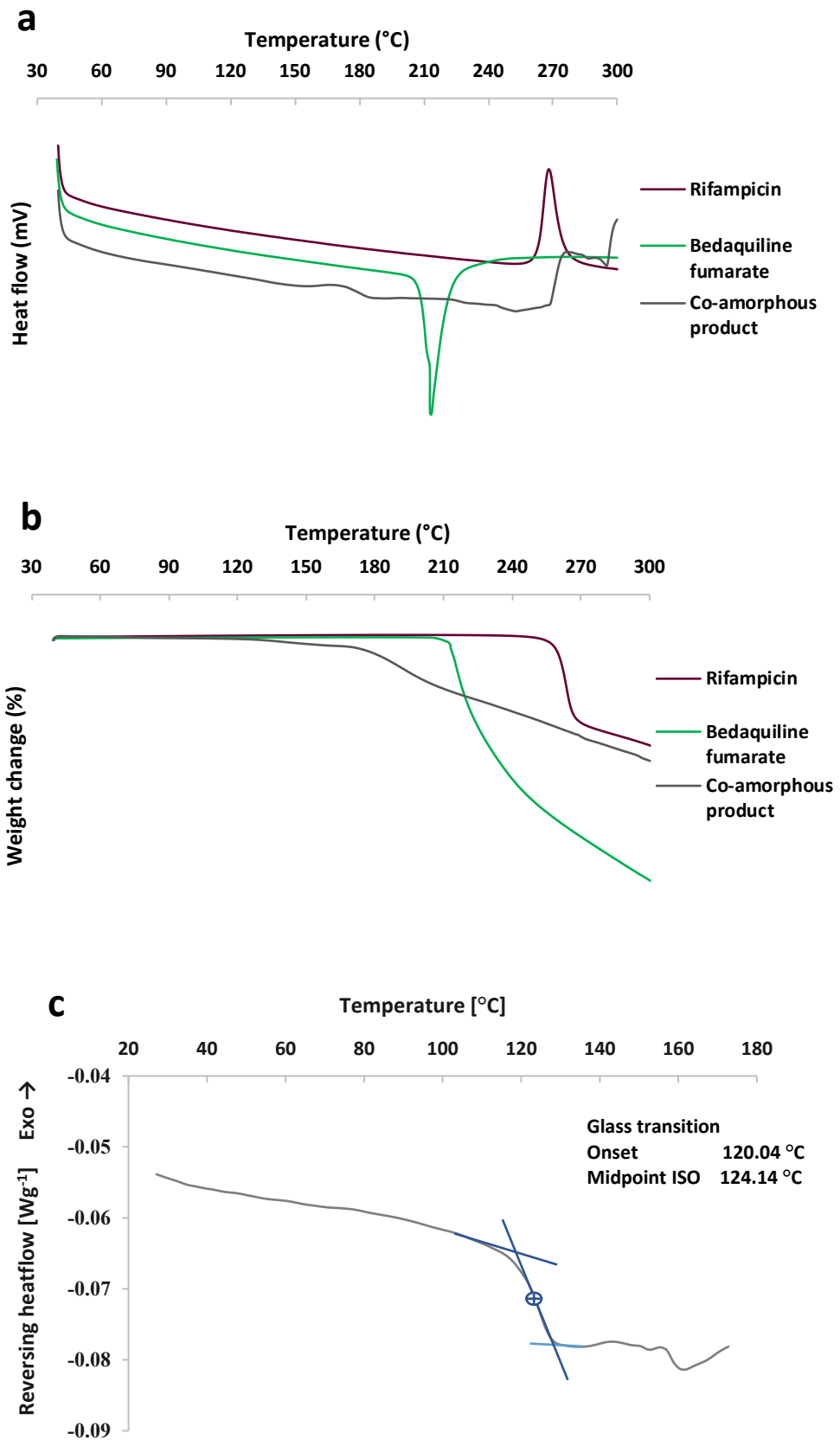

Figure 4. (**a**) DSC and (**b**) TGA thermograms of rifampicin, bedaquiline fumarate, and the rifampicin-bedaquiline fumarate co-amorphous product; (**c**) MDSC thermogram of the rifampicin-bedaquiline fumarate co-amorphous product.

 doi:10.20944/preprints202604.1177.v1

To further examine the product, modulated DSC was carried out. Based on the MDSC thermogram (**Figure 4c**), the material exhibits a single glass transition (Tg), with an onset at 120.49 °C and a midpoint at 124.44 °C. The presence of one well defined Tg indicates that the two drug molecules formed a single homogeneous co-amorphous phase, rather than existing as separate amorphous components, which would typically produce two distinct glass transitions. The absence of any melting endotherms or crystallization events further confirms the fully amorphous nature of the sample. Together, these thermal characteristics provide strong evidence that the material is a co amorphous system, with rifampicin and bedaquiline fumarate molecularly mixed at the amorphous level.

3.1.4. FTIR Spectra Results

Spectroscopic analysis of the samples was performed by FTIR (**Figure 5**). The rifampicin spectra showed characteristic peaks for polymorph I. These include sharp ansa OH peak at 3480 cm^{-1}, furanone C=O at 1644 cm^{-1}, single acetyl C=O peak at 1725 cm^{-1} and N-CH_3 stretching band at 2878 cm^{-1} [33]. Bedaquiline fumarate FTIR spectrum showed characteristic O-H stretching vibrations of alcohol group peaks at 3837, 3738, 3618 and 3245 cm^{-1}. Moreover, peaks at 2945, 2754 and 2604 cm^{-1} were representative of the fumarate salt carboxylic acid groups' O-H stretching. The C-H bending and stretching vibration peaks at 1458-1386 cm^{-1} and 3059.18 cm^{-1}, respectively. Other vibrations were observed including C-O bending at 2353 cm^{-1}, aromatic ring C=C stretching at 1548.64 cm^{-1}, C=O stretching peaks at 1701 and 1635 cm^{-1}. The characteristic aromatic amine C-N stretching peaks ranging from 1248.74 to 1055.89 cm^{-1}, and C-Br vibrations bands at 776, 699 and 638 cm^{-1}. These observations are in agreement with those previously reported in the literature [32,34].

Rifampicin-bedaquiline fumarate co-amorphous product showed significantly different FTIR spectra, with some indisputable changes. The peak assigned to the O-H stretching of carboxylic acid in the fumarate salt is broadened and lower in intensity, as well as other vibrations which are broadened that is typical for amorphous solids. (**Figure 5**).

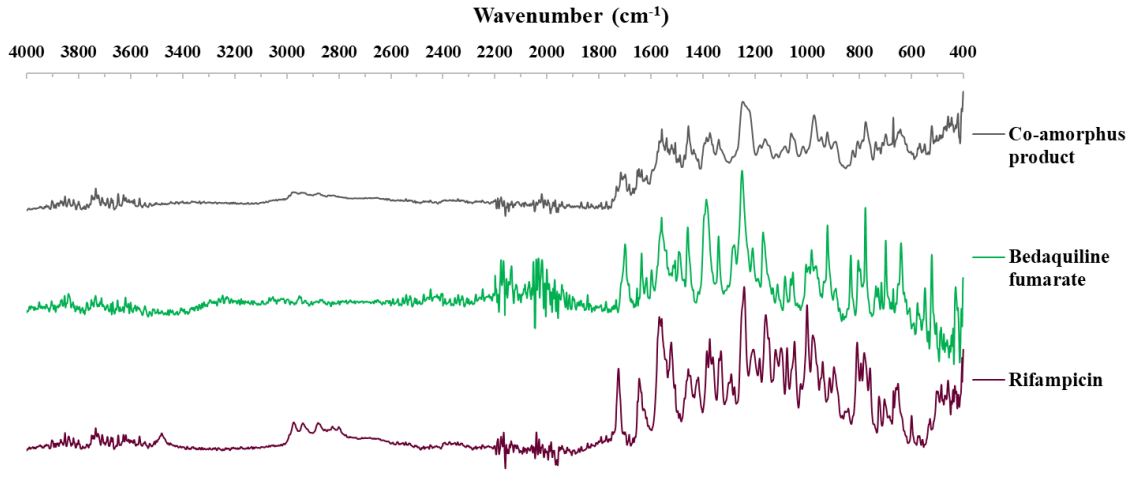

Figure 5. Normalized FTIR spectra of rifampicin, bedaquiline fumarate, and the rifampicin-bedaquiline fumarate co-amorphous product.

3.2. Dissolution

Dissolution of APIs are similar to those published in the literature for rifampicin [33] and bedaquiline fumarate [32]. The dissolution of both APIs within the co-amorphous product are presented separately in **Figure 6**. The rifampicin-bedaquiline fumarate co-amorphous product had significantly enhanced dissolution of the bedaquiline component (CAMP-bedaquiline) compared to the pure bedaquiline fumarate (p-value = 0.003, 0.012, <0.001, <0.001 and <0.001 at 10, 20, 30, 45 and

 doi:10.20944/preprints202604.1177.v1

60 minutes, respectively) (**Figure 6**). On the other hand, the dissolution of rifampicin from the co-amorphous product (CAMP-rifampicin) was only statistically lower at the beginning (from 10 to 30 minutes, *p*-values = >0.001, 0.007, and 0.005) compared to pure rifampicin. Then, there is no statistical difference in the dissolution after that (at 45 and 60 minutes). These results indicate that there was a statistical improvement in bedaquiline dissolution when formulated as a co-amorphous product, while there was no change to rifampicin dissolution.

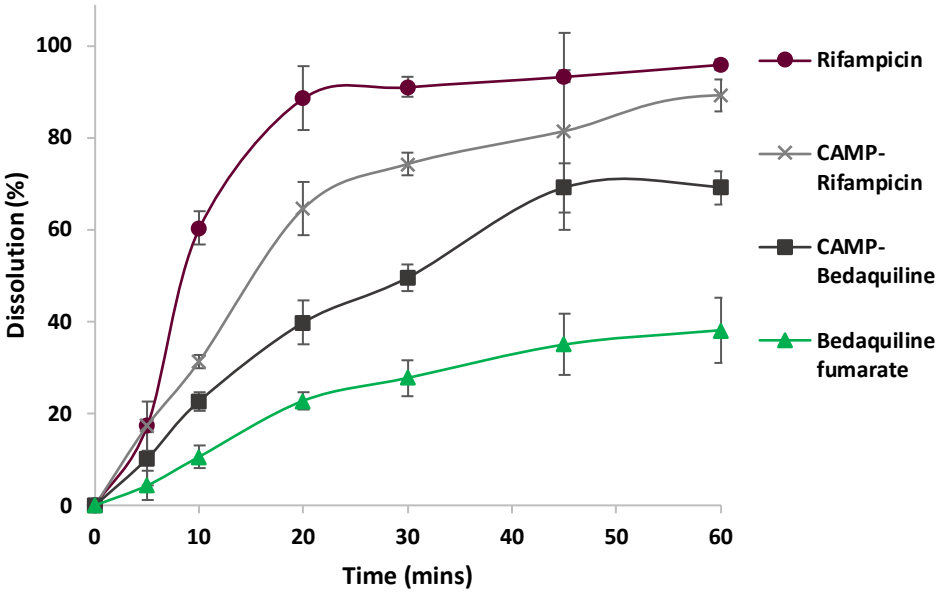

Figure 6. Dissolution profiles of the APIs and co-amorphous product (CAMP) of rifampicin and bedaquiline.

3.3. Accelerated Stability Study Results

The PXRD results of the accelerated stability study show the same pattern of intensity with no signs of recrystallization or structural transformation, confirming that the co-amorphous product remained physically stable under stress conditions (**Figure 7**). The difference in intensity observed in the fresh sample corresponds to the amount of sample used for the analysis, rather than structural changes. The diffractogram at stability conditions after 30 days does not have sharp peaks indicating crystalline structure or change in pattern. The co-amorphous product has not recrystallized or decomposed during the accelerated stability study. Product remained completely amorphous, supporting its potential for pharmaceutical development.

The collected analytical data strongly supports the formation of a co-amorphous system. Although the DSC thermogram (**Figure 4a**) suggests a potential glass transition near 160°C, its overlap with a minor mass loss in the TGA curve complicates definitive interpretation, possibly indicating residual solvent evaporation rather than a true glass transition. The absence of a melting peak for crystalline bedaquiline fumarate and the elevated thermal decomposition temperature point to strong intermolecular interactions, which are hallmarks of an co-amorphous systems. Additionally, modulated DSC (**Figure 4c**) shows a single, well-defined glass transition (Tg onset 120.49 °C; midpoint 124.44 °C) with no melting or crystallization events, providing further evidence for the formed a rifampicin and bedaquiline fumarate co-amorphous system with molecular-level mixing. These findings are further supported by the high morphological uniformity observed in SEM images (**Figure 2c**), which show no signs of phase separation or compositional variation, and the remarkable physical stability of the amorphous product under accelerated conditions (**Figure 7**). If multiple phases were present, instability would be expected in at least one component. Taken together, these findings indicate the formation of a single-phase, stable co-amorphous system.

 doi:10.20944/preprints202604.1177.v1

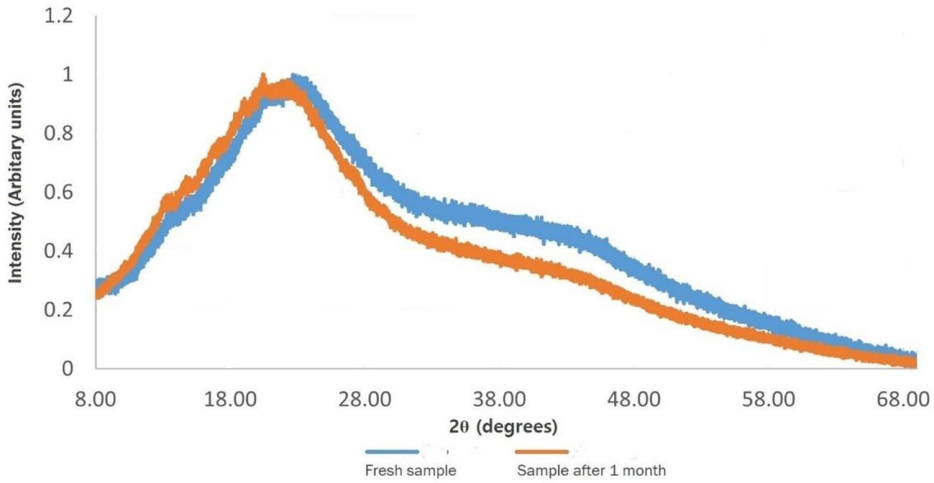

Figure 7. PXRD of the fresh sample and sample after 30 days.

4. Conclusions

The control of multidrug resistant tuberculosis is challenging. Bedaquiline fumarate and rifampicin are used to treat multidrug-resistant tuberculosis. However, the co-administration of rifampicin with bedaquiline has been reported to decrease the bioavailability of bedaquiline. In this study, a co-amorphous drug-drug delivery system comprising rifampicin and bedaquiline fumarate was successfully prepared using the fast solvent evaporation method. The resulting formulation exhibited a notably enhanced dissolution rate of bedaquiline, without compromising the dissolution rate of rifampicin or solid-state stability of the product under accelerated conditions for one month. These findings suggest that co-amorphous systems may offer a promising approach to improve the oral bioavailability of poorly soluble anti-tubercular drugs and potentially reduce the pill burden in multidrug resistant tuberculosis. Future studies, including detailed *in vitro-in vivo* correlation and bioavailability assessments, are needed to confirm the clinical utility of this formulation strategy and enable the use of such formulation in management of multidrug resistant tuberculosis.

Supplementary Materials: The following supporting information can be downloaded at: Preprints.org: **Table S1.** Hansen solubility parameters calculations for solvent selection calculations. **Figure S1**. Spectral properties of rifampicin, bedaquiline, and their equimolar mixture; **Figure S2.** Absorbance of (**a**) rifampicin and (**b**) bedaquiline at different concentrations; **Figure S3**. Calibration curves of (**a**) rifampicin at 225 and 334nm and (**b**) bedaquiline at 225nm.

Author Contributions: Conceptualization, A.S. and A.Sz; methodology, N.K., and S.N.; software, A.S., E.S., P.Z., A.Sz and T.B.; validation, A.Sz.; investigation, N.K., E.S.; data curation, N.K., E.S., P.Z., T.B., and S.N.; writing—original draft preparation, N.K., A.S.; writing—review and editing, P.S., A.Sz.; supervision, A.S.; project administration, A.Sz. All authors have read and agreed to the published version of the manuscript.

Funding: This research received no external funding.

Data Availability Statement: Not applicable.

Acknowledgments: The authors acknowledge János Kovács at the Environmental Analytical & Geoanalytical Research Group at the University of Pécs for the PXRD measurements and insightful discussions. The support of the academic and technical staff at the University of Pécs

Conflicts of Interest: The authors declare no conflict of interest.

 doi:10.20944/preprints202604.1177.v1

Abbreviations

The following abbreviations are used in this manuscript:

API	Active pharmaceutical ingredient
DSC	Differential scanning calorimetry
HSPs	Hansan solubility parameters
LD	Linear dichroism
PXRD	Powder x-ray diffraction
Ra	Modified radius
SEM	Scanning electron microscopy
TB	Tuberculosis
TGA	Thermogravimetric analysis

References

1. WHO (World Health Organization), "Global tuberculosis report 2023," Geneva, 2023.
2. S. Pallett and A. Houston, "Tuberculosis," *Medicine*, vol. 49, no. 12, pp. 751–755, 2021, doi: https://doi.org/10.1016/j.mpmed.2021.09.005.
3. J. Furin, H. Cox, and M. Pai, "Tuberculosis," *The Lancet*, vol. 393, no. 10181, pp. 1642–1656, Apr. 2019, doi: 10.1016/S0140-6736(19)30308-3.
4. J. Martínez-Campreciós, J. Espinosa-Pereiro, and A. Sánchez-Montalvá, "Update on the treatment of tuberculosis," *Medicina Clínica (English Edition)*, vol. 163, no. 5, pp. 245–252, 2024, doi: https://doi.org/10.1016/j.medcle.2024.02.016.
5. P. Desikan *et al.*, "Trends of drug resistance in M. tuberculosis in a reference laboratory in Central India: Forging ahead towards TB elimination," *Indian J Med Microbiol*, vol. 51, p. 100701, 2024, doi: https://doi.org/10.1016/j.ijmmb.2024.100701.
6. A. I. Zumla *et al.*, "New antituberculosis drugs, regimens, and adjunct therapies: needs, advances, and future prospects," *Lancet Infect Dis*, vol. 14, no. 4, pp. 327–340, Apr. 2014, doi: 10.1016/S1473-3099(13)70328-1.
7. J. P. Sarathy, G. Gruber, and T. Dick, "Re-Understanding the Mechanisms of Action of the Anti-Mycobacterial Drug Bedaquiline," *Antibiotics*, vol. 8, no. 4, p. 261, Dec. 2019, doi: 10.3390/antibiotics8040261.
8. M. Okezue *et al.*, "Crystal structures of salts of bedaquiline," *Acta Crystallogr C Struct Chem*, vol. 76, no. 11, pp. 1010–1023, Nov. 2020, doi: 10.1107/S2053229620013455.
9. S. Khoshnood *et al.*, "Bedaquiline: Current status and future perspectives," *J Glob Antimicrob Resist*, vol. 25, pp. 48–59, 2021, doi: https://doi.org/10.1016/j.jgar.2021.02.017.
10. A. Nusrath Unissa and L. E. Hanna, "Molecular mechanisms of action, resistance, detection to the first-line anti tuberculosis drugs: Rifampicin and pyrazinamide in the post whole genome sequencing era," *Tuberculosis*, vol. 105, pp. 96–107, Jul. 2017, doi: 10.1016/j.tube.2017.04.008.
11. W. Wehrli, "Rifampin: Mechanisms of Action and Resistance," *Clinical Infectious Diseases*, vol. 5, no. Supplement_3, pp. S407–S411, Jul. 1983, doi: 10.1093/clinids/5.Supplement_3.S407.
12. R. S. Wallis *et al.*, "Mycobactericidal activity of bedaquiline plus rifabutin or rifampin in ex vivo whole blood cultures of healthy volunteers: A randomized controlled trial," *PLoS One*, vol. 13, no. 5, p. e0196756, May 2018, doi: 10.1371/journal.pone.0196756.
13. E. M. Svensson, S. Murray, M. O. Karlsson, and K. E. Dooley, "Rifampicin and rifapentine significantly reduce concentrations of bedaquiline, a new anti-TB drug," *Journal of Antimicrobial Chemotherapy*, vol. 70, no. 4, pp. 1106–1114, Apr. 2015, doi: 10.1093/jac/dku504.
14. A. Younoussa *et al.*, "Protocol, rationale and design of BE-PEOPLE (Bedaquiline enhanced exposure prophylaxis for LEprosy in the Comoros): a cluster randomized trial on effectiveness of rifampicin and bedaquiline as post-exposure prophylaxis of leprosy contacts," *BMC Infect Dis*, vol. 23, no. 1, p. 310, May 2023, doi: 10.1186/s12879-023-08290-0.

 doi:10.20944/preprints202604.1177.v1

15. P. O. Campbell, N. M. Douglas, and S. T. Chambers, "A Review of the Efficacy, Safety, and Feasibility of Rifamycin-Based Post-Exposure Chemoprophylaxis for Leprosy," *Trop Med Infect Dis*, vol. 10, no. 4, p. 84, Mar. 2025, doi: 10.3390/tropicalmed10040084.
16. A. B. Buya *et al.*, "Application of Lipid-Based Nanocarriers for Antitubercular Drug Delivery: A Review," *Pharmaceutics*, vol. 13, no. 12, p. 2041, Nov. 2021, doi: 10.3390/pharmaceutics13122041.
17. J. Liu, H. Grohganz, K. Löbmann, T. Rades, and N.-J. Hempel, "Co-Amorphous Drug Formulations in Numbers: Recent Advances in Co-Amorphous Drug Formulations with Focus on Co-Formability, Molar Ratio, Preparation Methods, Physical Stability, In Vitro and In Vivo Performance, and New Formulation Strategies," *Pharmaceutics*, vol. 13, no. 3, p. 389, Mar. 2021, doi: 10.3390/pharmaceutics13030389.
18. E. FUKUOKA, M. MAKITA, and S. YAMAMURA, "Glassy State of Pharmaceuticals. III. : Thermal Properties and Stability of Glassy Pharmaceuticals and Their Binary Glass Systems," *Chem Pharm Bull (Tokyo)*, vol. 37, no. 4, pp. 1047–1050, 1989, doi: 10.1248/cpb.37.1047.
19. A. Saberi *et al.*, "Development, recent advances, and updates in binary, ternary co-amorphous systems, and ternary solid dispersions," *J Drug Deliv Sci Technol*, vol. 86, p. 104746, 2023, doi: https://doi.org/10.1016/j.jddst.2023.104746.
20. S.-H. Wang *et al.*, "Hansen solubility parameter analysis on the dispersion of zirconia nanocrystals," *J Colloid Interface Sci*, vol. 407, pp. 140–147, 2013, doi: https://doi.org/10.1016/j.jcis.2013.07.001.
21. M. A. Mohammad, A. Alhalaweh, and S. P. Velaga, "Hansen solubility parameter as a tool to predict cocrystal formation," *Int J Pharm*, vol. 407, no. 1, pp. 63–71, 2011, doi: https://doi.org/10.1016/j.ijpharm.2011.01.030.
22. A. Salem, S. Nagy, S. Pál, and A. Széchenyi, "Reliability of the Hansen solubility parameters as co-crystal formation prediction tool," *Int J Pharm*, vol. 558, pp. 319–327, 2019, doi: https://doi.org/10.1016/j.ijpharm.2019.01.007.
23. M. Á. Peña and F. Martínez, "Hansen Solubility Parameters: A Tool for Solvent Selection in Drugs," *Pharm Sci*, vol. 29, no. 2, pp. 133–134, 2023, doi: 10.34172/PS.2022.42.
24. G. Korshin, C. W. K. Chow, R. Fabris, and M. Drikas, "Absorbance spectroscopy-based examination of effects of coagulation on the reactivity of fractions of natural organic matter with varying apparent molecular weights," *Water Res*, vol. 43, no. 6, pp. 1541–1548, Apr. 2009, doi: 10.1016/j.watres.2008.12.041.
25. International Council for Harmonization, "Guidance for Industry Q1A(R2) Stability Testing of New Drug Substances and Products," Nov. 2003.
26. C. Singh, T. D. Bhatt, M. S. Gill, and S. Suresh, "Novel rifampicin–phospholipid complex for tubercular therapy: Synthesis, physicochemical characterization and in-vivo evaluation," *Int J Pharm*, vol. 460, no. 1–2, pp. 220–227, Jan. 2014, doi: 10.1016/j.ijpharm.2013.10.043.
27. B. Rangnekar, M. A. M. Momin, B. B. Eedara, S. Sinha, and S. C. Das, "Bedaquiline containing triple combination powder for inhalation to treat drug-resistant tuberculosis," *Int J Pharm*, vol. 570, p. 118689, Oct. 2019, doi: 10.1016/j.ijpharm.2019.118689.
28. V. Parvathaneni *et al.*, "Repurposing Bedaquiline for Effective Non-Small Cell Lung Cancer (NSCLC) Therapy as Inhalable Cyclodextrin-Based Molecular Inclusion Complexes," *Int J Mol Sci*, vol. 22, no. 9, p. 4783, Apr. 2021, doi: 10.3390/ijms22094783.
29. I. Ivanisevic, R. B. McClurg, and P. J. Schields, "Uses of <scp>X</scp> -Ray Powder Diffraction In the Pharmaceutical Industry," in *Pharmaceutical Sciences Encyclopedia*, Wiley, 2010, pp. 1–42. doi: 10.1002/9780470571224.pse414.
30. P. Khadka, P. C. Hill, B. Zhang, R. Katare, J. Dummer, and S. C. Das, "A study on polymorphic forms of rifampicin for inhaled high dose delivery in tuberculosis treatment," *Int J Pharm*, vol. 587, p. 119602, Sep. 2020, doi: 10.1016/j.ijpharm.2020.119602.
31. R. Alves, T. V. da S. Reis, L. C. C. da Silva, S. Storpírtis, L. P. Mercuri, and J. do R. Matos, "Thermal behavior and decomposition kinetics of rifampicin polymorphs under isothermal and non-isothermal conditions," *Brazilian Journal of Pharmaceutical Sciences*, vol. 46, no. 2, pp. 343–351, Jun. 2010, doi: 10.1590/S1984-82502010000200022.

 doi:10.20944/preprints202604.1177.v1

32. V. P. Pardhi and K. Jain, "Impact of binary/ternary solid dispersion utilizing poloxamer 188 and TPGS to improve pharmaceutical attributes of bedaquiline fumarate," *J Drug Deliv Sci Technol*, vol. 62, p. 102349, 2021, doi: https://doi.org/10.1016/j.jddst.2021.102349.
33. S. Agrawal, Y. Ashokraj, P. V Bharatam, O. Pillai, and R. Panchagnula, "Solid-state characterization of rifampicin samples and its biopharmaceutic relevance," *European Journal of Pharmaceutical Sciences*, vol. 22, no. 2–3, pp. 127–144, Jun. 2004, doi: 10.1016/j.ejps.2004.02.011.
34. Jinyi XULiang ZhangXiangyang ZhangXinzeng WANGJian CHAIHongying LUOZhiqing YANG, "Crystalline forms of bedaquiline fumarate and preparation methods therefor," EP3366676B1, 2021